Int. J. Electrochem. Sci., 12 **(2017)** 166 – 177, doi: 10.20964/2017.01.04

International Journal of
ELECTROCHEMICAL
SCIENCE
www.electrochemsci.org

Synergistic Effect of Potassium Iodide with L-Tryptophane on the Corrosion Inhibition of Mild Steel: A Combined Electrochemical and Theoretical Study

Lei Guo[1,*], *Guang Ye*[1], *Ime Bassey Obot*[2], *Xiaohong Li*[1], *Xun Shen*[1], *Wei Shi*[1], *Xingwen Zheng*[3]

[1] School of Material and Chemical Engieering, Tongren University, Tongren 554300, China
[2] Center of Research Excellence in Corrosion, King Fahd University of Petroleum and Minerals, Dhahran 31261, Saudi Arabia
[3] Material Corrosion and Protection Key Laboratory of Sichuan province, Zigong 643000, China
[*]E-mail: cqglei@163.com

Received: 30 September 2016 / *Accepted:* 8 Nobember 2016 / *Published:* 12 December 2016

The inhibition effects of L-tryptophane (Trp) and its synergistic effect with KI on the corrosion of mild steel in 1.0 M HCl solution have been investigated by electrochemical impedance spectroscopy (EIS) and potentiodynamic polarization (PDP) measurements. The results show that the inhibition efficiency increases with the concentration of Trp and increases further when KI exists. The synergistic effect between Trp and KI was discussed by calculating the synergism parameter, which suggests that there is a cooperative mechanism between iodide anion and Trp cation. Finally, Monte Carlo simulation was utilized to search for the equilibrium configurations of inhibitors/Fe(110) adsorption systems in the presence of water molecules.

Keywords: L-tryptophane, Corrosion inhibitor, Mild steel, Theoretical calculations, Electrochemical investigation

1. INTRODUCTION

Due to the good mechanical performance and low price, mild steel is widely used as the construction and engineering materials in a variety of industrial applications such as pipes, storage tanks. However, they can be suffering severe corrosion damage in the bad corrosive environment during their service, which usually results in large economic losses and a number of security issues. So anticorrosion technology has attracted more and more researchers' attention [1, 2]. The most effective and convenient way to prevent steel from corrosion is the use of organic corrosion inhibitors [3]. The organic materials containing polar functions with N, O, and/or S atoms as well as aromatic rings have

been confirmed to exhibit good inhibiting performance [4]. So far, most researchers believe that most organic inhibitors can form a compact barrier which adheres to the substrate surface by displacing H_2O molecules [5-7].

Amino acids are a kind of very useful chemical substances to the health of mankind. They often contain amine ($–NH_2$) and carboxylic acid (–COOH) functional groups in the molecular structure. They are nontoxic, low price and easy to produce in purities greater than 99%. Some researchers have examined the inhibition effectiveness of many amino acids on the corrosion of metals recently [8-10]. One problem here is that the inhibitors studied are usually a single component, the report on the synergistic effect with other inorganic salt (such as KBr, KI) are still fewer. The importance of synergistic effect on inhibition in acid media is vast, because it can improve the inhibitive activities of the inhibitors with a small amount of usage, and extend their application areas. Many researches on synergistic effect have been carried out and are being investigated [11-14]. For example, Musa *et al.* [15] have studied the synergistic effect of KI with phthalazone on the corrosion inhibition of mild steel in 1.0 M HCl. They reported that the inhibition efficiency of adenine is greatly enhanced with the presence of KI due to the specific adsorption effect of iodide ions.

On the other hand, molecular modeling methods (quantum mechanics, Metropolis Monte Carlo method, *etc.*) have been applied to to explain anticorrosive mechanism [16-19]. Theoretical calculation has been considered an effective, reliable, advanced and low-cost way that is capable of successfully exploring the interaction of inhibitors with the metal surface or similar problems. Its major contribution is related to reducing the time and cost in exploring the inhibition mechanism as well as developing green organic corrosion inhibitors [20, 21].

In this work, the synergistic effect of potassium iodide (KI) and L-tryptophane (Trp) on the corrosion inhibition of mild steel in 1.0 M HCl has been studied by electrochemical methods and theoretical calculation technique. To facilitate the presentation, the molecular structure of Trp and the change pattern of its solubility with pH is presented in Figure 1. Careful inspection of Figure 1b we can see that Trp has a good solubility in strong acid media and may serve as a suitable material for corrosion inhibitor.

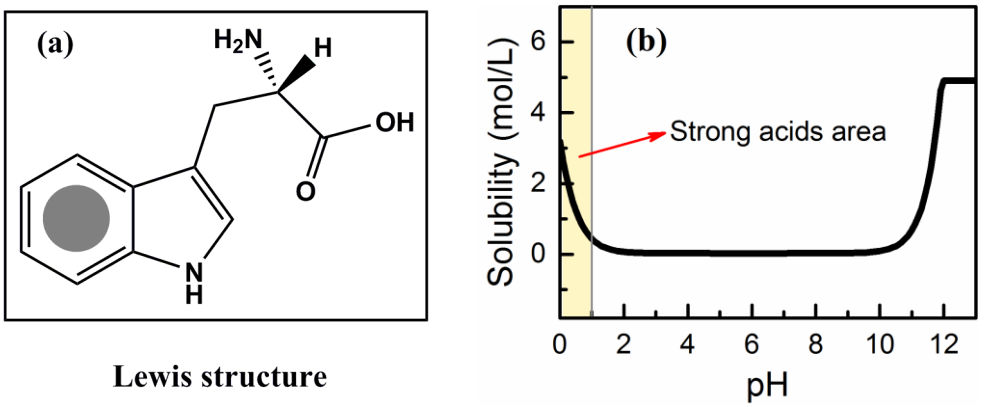

Figure 1. Molecular structure (a) and the solubility *vs.* pH (b) of L-tryptophane.

2. EXPERIMENTAL PROCEDURE

2.1. Materials and chemicals

The working electrode employed in this work is mild steel Q235 (the chemical composition is shown in Table 1). The steel rod was imbedded in epoxy resin with a surface area of (1.0 × 1.0) cm^2 exposed to the corrosive media. Prior to each experiment, the exposed surface was polished with 400#, 800#, 1000# and 1200# emery paper, washed thoroughly with deionized water, degreased and cleaned ultrasonically in ethanol and finally dried. The simulation medium (*i.e.*, 1.0 M HCl solution) was prepared by using hydrochloric acid of standard grade and doubly deionized water.

Table 1. Chemical composition of the Q235 mild steel (in wt%).

Elemental	C	Mn	Si	Cu	S	Fe
Compositions	0.17	0.46	0.26	0.019	0.017	Balance

2.2. Electrochemical measurements

RST5000F electrochemical system (Shiruisi Technology Co. Ltd., from China) was employed for all the electrochemical tests. A standard three-electrode system was used and the temperature was controlled at 298±1 K. The reference electrode was a saturated calomel electrode (SCE) provided with a Luggin-Haber capillary tip. A Platinum plate was used as the counter electrode. Primitively, the open circuit corrosion potential (OCP) test lasted about 1 h in order to attain a stable value. The impedance studies were carried out in the frequency range of 10^5 to 10^{-2} Hz at E_{ocp} by applying 10 mV amplitude. Obtained impedance data from EIS were calculated by using ZsimpWin 3.10 software. The Tafel polarization was performed in the potential range of ±250 mV *vs.* E_{ocp} at a scan rate of 0.5 mV/s. Each test was repeated at least three times in order to verify the reproducibility.

2.3. Theory and computation details

Density functional theory (DFT) calculations were conducted with $DMol^3$ module in Materials Studio (MS) software (version 8.0, from BIOVIA Inc.) [22]. The $DMol^3$ program uses numerical functions on an atom centered grid as its atomic basis, which is far more complete than the traditional Gaussian functions. Geometrical optimizations were performed by the generalized gradient approximation (GGA) functional of Becke exchange plus Lee-Yang-Parr correlation (BLYP) in conjunction with double numerical with polarization (DNP) basis set. The real space cutoff radius was 3.7 Å, and the choice of convergence accuracy was Fine. The optimized structures were confirmed to be true minima by vibrational frequency calculations. To get more reliable data, conductor-like screening model (COSMO) [23] was applied in order to incorporate the solvent effects (herein, water, dielectric constant = 78.54) in the calculation.

The interactions between the inhibitors of interest and the iron surface were simulated by applyling the adsorption locator module (also implemented in MS 8.0) through Metropolis Monte Carlo approach [24]. The calculation was carried out using the COMPASSII force field [25]. The Fe(110) plane was chosen in this work due to its stable property. It was first cleaved from bcc Fe crystal, and was then enlarged to a (8×8) supercell, after which a vacuum slab with 35 Å thickness was built above the Fe(110) plane. The optimized inhibitor molecule was put to adsorb on the refined Fe(110) surface with the aid of simulated annealing task to obtain equilibrium configuration of inhibitor/Fe(110) system. Finally, we can obtain the adsorption energy value for the most stable configuration of inhibitor/Fe(110) system. Moreover, each adsorption system also included 400 H_2O molecules to simulate the solvent effects. More details about the methodology of Monte Carlo simulations had been reported in our previous work [26-29].

3. RESULTS AND DISCUSSION

3.1. EIS studies

Nyquist impedance plots of mild steel in 1.0 M HCl solution containing different concentrations of Trp in the absence and presence of 5 × 10^{-3} M KI are given in Figure 2. We can see that all impedance spectra display a single depressed capacitive arc over the frequency range studied, and this is often considered to related to the charge-transfer process [30]. The capacitive arcs are not perfect semicircles, and this difference could be attributed to the frequency dispersion as results of the roughness and inhomogeneous of electrode surface [31-33]. With the concentration of inhibitors increasing, the capacitive reactance arc radius became larger.

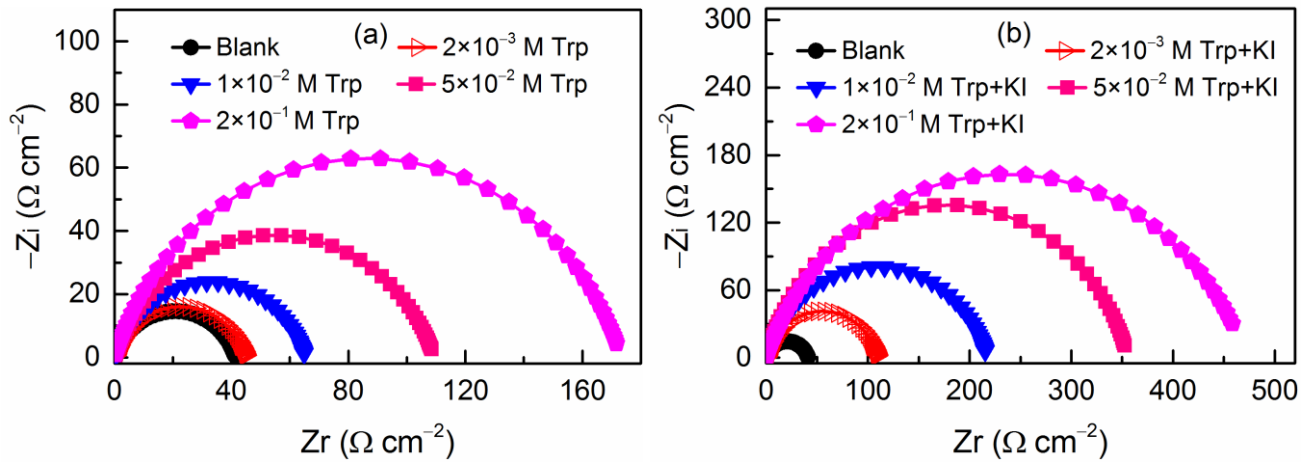

Figure 2. Nyquist plots for mild steel in 1.0 M HCl containing various concentrations of Trp in the (a) absence, and (b) presence of 5 × 10^{-3} M KI.

The Randles equivalent circuit (Figure 3) model was used. R_{ct} is the charge transfer resistance, R_s is the solution resistance, and CPE represents a constant phase element. CPE has the value of the frequency-distributed double-layer capacitance. The impedance function of the CPE has the form [34]

$$Z_{CPE} = \frac{1}{Y_0(j\omega)^n} \quad (1)$$

where Y_0 is a proportionality coefficient, j is the imaginary number, ω is the angular frequency ($\omega=2\pi f$, here f is the AC frequency in Hz), and n is a phase shift, which is related to the system homogeneity. When the CPE represents a pure capacitor, n=1. The capacitance values (C_{dl}) and inhibition efficiency (η_R) can be calculated as follow:

$$C_{dl} = \frac{Y_0\omega^{n-1}}{\sin(n\pi/2)} \quad (2)$$

$$\eta_R = \frac{R_{ct(inh)} - R_{ct(0)}}{R_{ct(inh)}} \times 100 \quad (3)$$

where $R_{ct(0)}$ and $R_{ct(inh)}$ are the charge transfer resistance in the absence and presence of inhibitors, respectively. The fitted impedance data such as R_s, R_{ct} and CPE constants Y_0 and n are listed in Table 2.

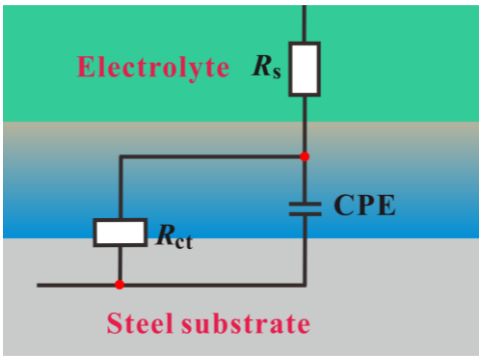

Figure 3. Equivalent circuit used to fit the EIS data.

Table 2. Impedance parameters of mild steel in 1.0 M HCl with different concentrations of Trp in the presence and absence of KI.

C (M)		R_s (Ω cm^2)	CPE		R_{ct} (Ω cm^2)	C_{dl} (μF cm^{-2})	η_R
C_{Trp} (M)	C_{KI} (M)		Y_0 ($\times10^{-5}$ S s^n cm^{-2})	n			
Blank	/	0.154	55.5	0.775	41.2	557	/
Blank	5×10^{-3}	0.115	25.6	0.797	102.3	279	59.7
2×10^{-3}	/	0.148	53.5	0.788	46.9	538	12.1
2×10^{-3}	5×10^{-3}	0.164	25.2	0.821	113.6	281	63.7
1×10^{-2}	/	0.151	41.8	0.806	65.8	436	37.3
1×10^{-2}	5×10^{-3}	0.061	19.7	0.813	225.7	248	81.7
5×10^{-2}	/	0.097	33.6	0.795	109.4	381	62.3
5×10^{-2}	5×10^{-3}	0.043	13.5	0.829	355.8	169	88.4
2×10^{-1}	/	0.098	22.8	0.801	173.1	252	76.1
2×10^{-1}	5×10^{-3}	0.035	13.1	0.814	509.1	138	91.9

As seen in Table 2, the R_{ct} values increased considerably after the addition of inhibitors, and they continuously increased as inhibitor concentration increases and hence an increase in inhibition efficiency. This can be attributed to the formation of an insulating layer on the iron surface, which forms a barrier for mass and charge-transfer at the electrode surface [35]. The thickness of the barrier layer (d) is related to C_{dl}, *i.e.*, $C_{dl}=(\varepsilon_0\varepsilon S)/d$. Apparently the C_{dl} values strongly decreased with increasing inhibitor concentration, which resulted from a decrease in the local dielectric constant ε and/or an increase in the thickness of the electrical double layer, suggesting that the inhibitor strongly adsorbed to the metal/solution interface [36]. The addition of KI can further enhance R_{ct} values and reduces C_{dl} values, which may be caused to the enhanced adsorption of Trp in the presence of KI since the synergistic effect with iodide ions. The best corrosion inhibition efficiency is 91.9% when the concentration of Trp is 0.2 M in the presence of KI.

3.2. PDP measurements

The representative polarization curves for mild steel in 1.0 M HCl solution with different concentrations of Trp in the presence and absence of 5 × 10^{-3} M KI was shown in Figure 4. Some electrochemical corrosion parameters, specifically, corrosion potential (E_{corr}), corrosion current density (i_{corr}), cathodic and anodic tafel slopes (β_c, β_a) obtained from the polarization measurements were summarized in Table 2. The inhibition efficiency (η_p) was calculated by using the formula:

$$\eta_p = \frac{i_{corr(0)} - i_{corr(inh)}}{i_{corr(0)}} \times 100 \qquad (4)$$

where $i_{corr(0)}$ and $i_{corr(inh)}$ are the corrosion current density of mild steel in the absence and presence of inhibitors, respectively. The i_{corr} values were determined by extrapolation of the linear segments of the anodic and cathodic Tafel curves.

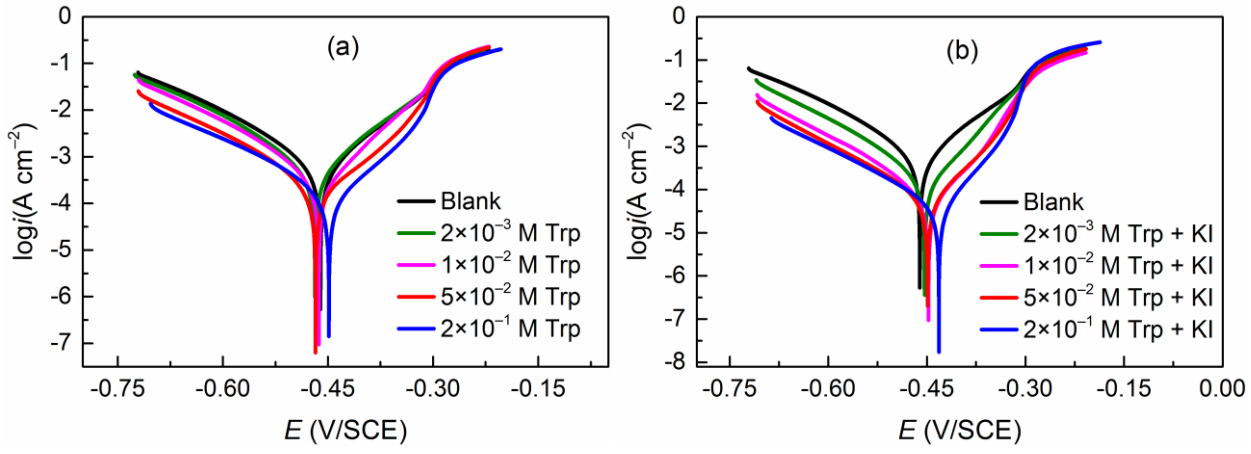

Figure 4. Potentiodynamic polarization curves for mild steel in 1.0 M HCl containing various concentrations of Trp in the (a) absence, and (b) presence of 5 × 10^{-3} M KI.

From the results in Figure 4 and Table 3, it is observed that the corrosion current (i_{corr}) was found to decrease with increaseing inhibitor concentration. The addition of Trp inhibitor not only reduces anodic dissolution of Fe ($Fe–2e^{-}\rightarrow Fe^{2+}$), but also inhibits cathodic hydrogen evolution reaction ($2H^{+}+2e^{-}\rightarrow H_2$). We can also conclude that the addition of KI further reduces the i_{corr} values and improves the inhibition efficiency of Trp significantly. The inhibition efficiency derived from polarization measurements are in good agreement with that from EIS. This proves that the data obtained form the electrochemical method is reliable.

Table 3. PDP parameters for mild steel in 1.0 M HCl with different concentrations of Trp in the presence and absence of KI.

C_{Trp} (M)	C_{KI} (M)	E_{corr}(mV)	i_{corr} (μA cm^{-2})	β_c (V dec^{-1})	β_a (mV dec^{-1})	η_p	S
Blank	/	−460	514.3	0.10	0.08	/	/
Blank	5×10^{-3}	−457	231.0	0.09	0.06	55.0	/
2×10^{-3}	/	−468	421.9	0.09	0.08	17.9	/
2×10^{-3}	5×10^{-3}	−452	180.9	0.09	0.05	64.8	1.047
1×10^{-2}	/	−463	304.7	0.09	0.06	40.7	/
1×10^{-2}	5×10^{-3}	−447	84.8	0.09	0.05	83.5	1.613
5×10^{-2}	/	−467	210.7	0.10	0.08	59.1	/
5×10^{-2}	5×10^{-3}	−441	56.7	0.11	0.06	88.9	1.669
2×10^{-1}	/	−448	139.7	0.11	0.07	72.8	/
2×10^{-1}	5×10^{-3}	−431	38.5	0.11	0.05	92.5	1.629

The interaction between KI and Trp molecules can be described by introduction of an S synergism parameter, which is defined as

$$S = \frac{I_1 \times I_2}{I_{1,2} \times I_0} \qquad (5)$$

Herein, I_1 and I_2 are the corrosion current density for single KI and Trp, respectively. $I_{1,2}$ is the obtained corrosion current density for the Trp + KI containing solution, I_0 is the corrosion current density for the blank solution. Generally, if the values of $S < 1$ indicates that antagonistic effect prevails which may lead to competitive adsorption, whereas $S > 1$ suggests a synergistic effect [37]. The calculated synergism parameters are listed in Table 3. We find that the values of S are more than 1, which suggests a cooperative synergistic effect exists. That is, iodide ions were firstly adsorbed onto the positively charged metallic surface (Fe^{2+}), followed by adsorption of Trp cations (TrpH) on the layer of KI anions.

According to the literature and other authors' results in research works [38, 39], if the E_{corr} (inhibitor) displacement is lower than 85 mV respect to E_{corr} (blank), the inhibitor can act as amixed type. In the presence study, the maximum displacement is 29 mV, which suggests that investigated compounds act as mixed type inhibitors.

3.3. Theoretical study

Actually, Trp is an amphoteric compound, the $-NH_2$ (pK_a=7.97, calculated from ACD/Labs) part of the Trp molecule is easily to be protonated and form the cationic forms in acid media, and the protonation process is shown in Figure 5. Then its protonated form (abbreviated as TrpH) was considered in the following theoretical calculations.

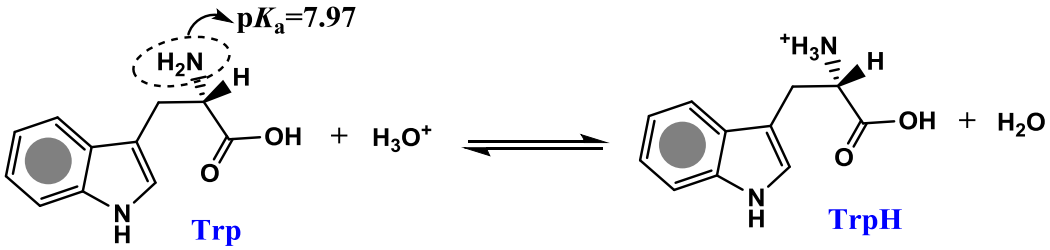

Figure 5. The protonation process of a Trp molecule in acidic solution.

3.3.1. Quantum chemical calculations

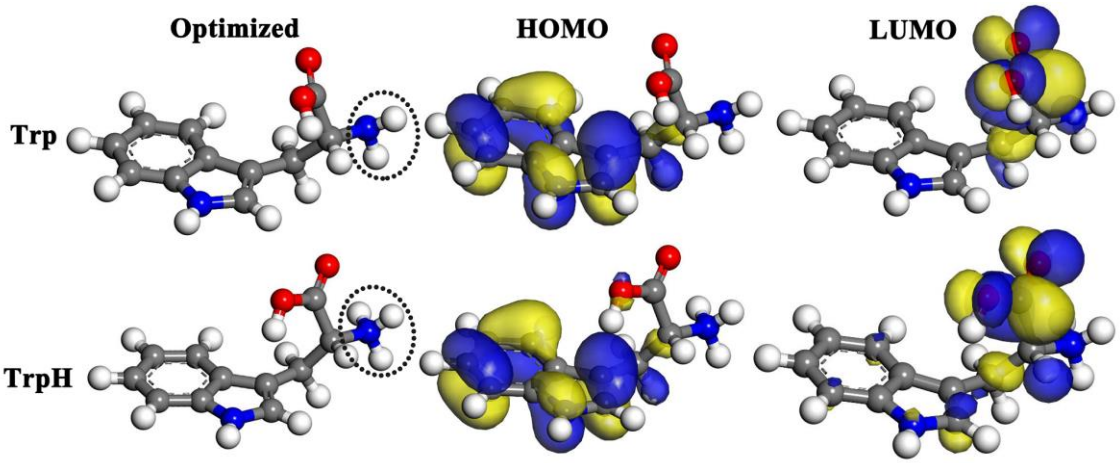

Figure 6. Optimized geometric structures and molecular orbitals for Trp and TrpH at the GGA/BLYP/DNP level of theory.

The optimized geometric structures as well as frontier molecular orbital distributions for neutral and protonated forms of Trp are shown in Figure 6. The HOMO of Trp shows the electron density contributed from indole ring, while the LUMO finds predominant contribution from the nitrogen atom of amine group as well as the carboxyl oxygen atoms. A similar delocalized electron density at the HOMO and LUMO of TrpH exists.

On the basis of Koopmans's theorem [40, 41], the negative of the HOMO energy ($-E_{HOMO}$) and the LUMO energy ($-E_{LUMO}$) correspond to the ionization potential and electron affinity, respectively (*i.e.*, $I = -E_{HOMO}$ and $A = -E_{LUMO}$). The quantum chemical descriptors electronegativity (χ) and hardness (η) are thereby defined as:

$$\chi = (I + A)/2 = -(E_{HOMO} + E_{LUMO})/2 \qquad (6)$$

$$\eta = (I - A)/2 = (E_{LUMO} - E_{HOMO})/2 \quad (7)$$

Based on Table 4, the E_{HOMO} and E_{LUMO} values for Trp molecule are more positive than TrpH, and the energy gap (ΔE) values for the former (3.52 eV) is also seen to be bigger than the latter (3.38 eV). Some researchers reported that lower value of ΔE is responsible for higher inhibition efficiency of inhibitors [42-44]. All this suggests that the dominant form responsible for the inhibition efficiency of Trp is its protonated form in an acidic medium.

Table 4. Calculated quantum chemical descriptors at the GGA/BLYP/DNP level for Trp and TrpH in aqueous phase.

Inhibitor	E_{HOMO} (eV)	E_{LUMO} (eV)	I (eV)	A (eV)	ΔE (eV)	χ (eV)	η (eV)	ΔN
Trp	–4.89	–1.36	4.89	1.36	3.52	3.12	1.76	1.09
TrpH	–5.25	–1.86	5.25	1.86	3.38	3.56	1.69	1.01

The fraction of electrons (ΔN) transferred between the inhibitor and metallic surface is given by

$$\Delta N = \frac{\chi_{Fe} - \chi_{inh}}{2(\eta_{Fe} + \eta_{inh})} \quad (8)$$

where a theoretical value of $\chi_{Fe} \approx 7$ eV, and $\eta_{Fe} = 0$ is taken based on the assumption that $I = A$ for a bulk metal, since they are softer than the neutral metallic atoms. The ΔN value measures the electron transfer from molecule to metal if $\Delta N > 0$ and vice versa if $\Delta N < 0$. Furthermore, Lukovits and others [17] point out that when $\Delta N < 3.6$, the inhibition efficiency increases with the ability of electrons donation to the metal surface. It can be seen from Table 3 that the ΔN value of Trp is slightly higher than that of TrpH molecule, but quite similar. Both of the ΔN values are positive, which demonstrates that Trp and TrpH can donate electrons to the iron surface to form self-assembled layers of inhibitors.

3.3.2. Monte Carlo Simulation

Recently, there is a perception that the analysis of molecular electronic structure of organic molecules is not sufficient to determine the trend of their corrosion inhibition performance [26, 45]. So it is necessary to carry out rigorous investigation of the direct interaction between the inhibitors and mild steel surface incorporating water molecules to simulate the actual environment. Thus, in the present study, Monte Carlo simulation was utilized to investigate the synergistic adsorption effect of Trp and KI on iron surface.

The equilibrium configurations of the inhibitors/Fe(110) systems are given in Figure 7. As shown in Figure 7a, the TrpH molecule adsorbed on Fe(110) surface in nearly parallel orientation. Figure 7b shows that there is an electrostatic interaction between iodine ions and Fe(110) surface. An examination of Figure 7c reveals that the I^- ions tend to attract the protonated nitrogen atom, and we can generalize it as a bridge joining the positively charged TrpH cations and the positively charged iron surface. The computed energy parameters of the equilibrium configurations of inhibitors/Fe(110) systems are given in Table 5. The large negative values of adsorption energy for all studied adsorption

systems suggest that the inhibitors are quickly and tightly adsorbed on the Fe(110) surface. The sequence of adsorption energy for the tested inhibitors was TrpH + I^- > TrpH > I^-. This trend agrees well with the order of inhibition efficiency mensurated from experiments.

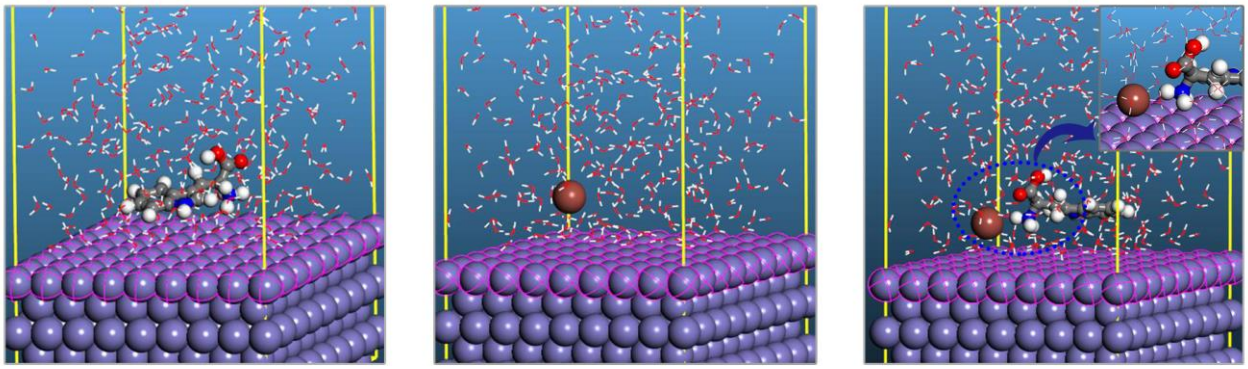

Figure 7. Snapshots of the most stable low energy configurations for the adsorption of (a) TrpH, (b) I^-, and (c) TrpH + I^- on Fe(110)/400 H_2O interface obtained through the Monte Carlo simulation.

Table 5. Outputs and descriptors calculated by the Mont Carlo simulation for the lowest adsorption configurations of (a) TrpH, (b) I^-, and (c) TrpH + I^- on Fe (110)/400 H_2O Interface (in $\times 10^3$ kcal mol^{-1}).

Systems	Total energy	Adsorption energy	Rigid adsorption energy	Deformation energy
Fe(110)/ I^-	–5.045	–12.76	–5.337	–7.431
Fe(110)/TrpH	–5.011	–12.80	–5.360	–7.444
Fe(110)/TrpH+ I^-	–5.092	–12.88	–5.442	–7.443

3.4. Mechanism of adsorption and inhibition

The inhibition mechanism of mild steel in HCl solution by Trp and KI can be explained as adsorption. But it is difficult to explain the single mode of adsorption because the adsorption of inhibitor cannot consider as purely physical or chemical type.

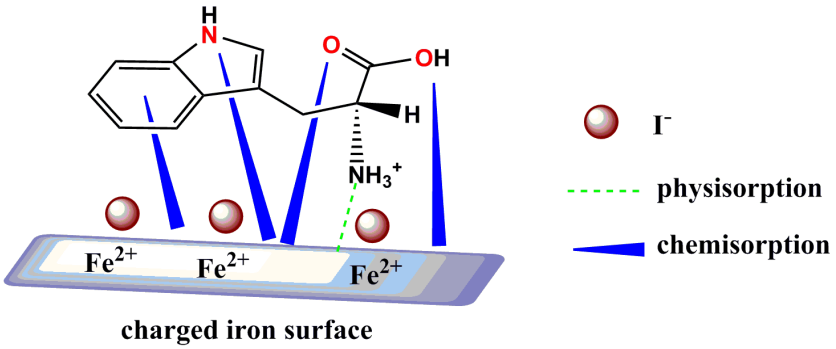

Figure 8. Schematic illustration of the adsorption model of inhibitors on mild steel surface in acid media.

The mechanism of adsorption can be explained according to the following ways shown in Figure 8.

(i) The Trp molecules exist in 1.0 M HCl as protonated species. They can get adsorbed on previously adsorbed I^- on the mild steel interface through electrostatic interaction (physisorption).

(ii) Trp molecule may be adsorbed on the iron surface *via* the chemisorptions mechanism through donation of lone electrons pairs of N atoms as well as O atoms to the empty orbital of Fe atoms.

(iii) There is donor–acceptor interactions between the π-electrons of aromatic ring and *d*-orbital of Fe atoms.

4. CONCLUSIONS

In the present work, the corrosion inhibition of Trp and KI for mild steel in 1.0 M HCl solution have been investigated by electrochemical and theoretical calculation methods. The main conclusions of this work are given below:

(1) The inhibition effectiveness of Trp was found to further increase with the addition of KI as a result of the synergistic effect. There is a cooperative synergistic mechanism between the iodide anion and Trp cation.

(2) The Trp molecule can absorb onto Fe(110) with the molecular plane being nearly parallel to the surface.

(3) The variation in the values of Tafel slopes and the minor displacement of E_{corr} with respect to E_{corr} of the blank indicate that the inhibitors of interest are mixed type in nature.

(4) Both physical and chemical adsorption are exist in the inhibition process.

ACKNOWLEDGEMENTS
This research was sponsored by the Science and Technology Program of Guizhou Province (No. QKH JC[2016]1149), the Guizhou Provincial Department of Education Fundation (No. QJHKYZ[2016] 105), the Opening Project of Material Corrosion and Protection Key Laboratory of Sichuan Province (No. 2016CL06), the Guizhou Provincial Department of Education 125 Major Project Fundation (No. QJH2013-027), the Research Fund for the Doctoral Program of Tongren University (No. trxyDH1510), and the student's platform for innovation and entrepreneurship training program (No. 2016106665).

References

1. X.G. Li, D.W. Zhang, Z.Y. Liu, Z. Li, C.W. Du, C.F. Dong, *Nature*, 527 (2015) 441-442.
2. A. Cook, G. Frankel, A. Davenport, T. Hughes, S. Gibbon, D. Williams, H. Bluhm, V. Maurice, S. Lyth, P. Marcus, D. Shoesmith, C. Wren, J. Wharton, G. Hunt, S. Lyon, T. Majchrowski, R. Lindsay, G. Williams, B. Rico Oller, M. Todorova, S. Nixon, S.T. Cheng, J. Scully, A. Wilson, F. Renner, Y.H. Chen, C. Taylor, H. Habazaki, A. Michaelides, S. Morsch, P. Visser, L. Kyhl, A. Kokalj, *Faraday Discuss.*, 180 (2015) 543-576.
3. B.E.A. Rani, B.B.J. Basu, *Int. J. Corros.*, 2012 (2012) 1-15.
4. P.B. Raja, M. Ismail, S. Ghoreishiamiri, J. Mirza, M.C. Ismail, S. Kakooei, A.A. Rahim, *Chem. Eng. Commun.*, 203 (2016) 1145-1156.
5. N. Kovacevic, A. Kokalj, *Mater. Chem. Phys.*, 137 (2012) 331-339.
6. J. Zhang, G. Qiao, S. Hu, Y. Yan, Z. Ren, L. Yu, *Corros. Sci.*, 53 (2011) 147-152.

7. A. Kokalj, *Faraday Discuss.*, 180 (2015) 415-438.
8. A. Aouniti, B. Hammouti, Y. Abed, S. Kertit, *Bull. Electrochem.*, 17 (2001) 13-17.
9. Z. Ghasemi, A. Tizpar, *Appl. Surf. Sci.*, 252 (2006) 3667-3672.
10. D.Q. Zhang, Q.R. Cai, X.M. He, L.X. Ga, G.D. Zhou, *Mater. Chem. Phys.*, 112 (2008) 353-358.
11. A.S. Yaro, A.A. Khadom, S.M. Lahmod, *React. Kinet. Mech. Cat.*, 109 (2013) 417-432.
12. J.C. Li, M. Zhao, Q. Jiang, *Mater. Performance*, 45 (2006) 42-44.
13. L. Larabi, Y. Harek, M. Traisnel, A. Mansri, *J. Appl. Electrochem.*, 34 (2004) 833-839.
14. S. Khan, M.A. Quraishi, *Arab. J. Sci. Eng.*, 35 (2010) 71-82.
15. A.Y. Musa, A. Mohamad, A.A.H. Kadhum, M.S. Takriff, L.T. Tien, *Corros. Sci.*, 53 (2011) 3672-3677.
16. G. Gece, *Corros. Sci.*, 50 (2008) 2981-2992.
17. I. Lukovits, E. Kalman, F. Zucchi, *Corrosion*, 57 (2001) 3-8.
18. C. Gattinoni, A. Michaelides, *Faraday Discuss.*, 180 (2015) 439-458.
19. S. Kaya, L. Guo, C. Kaya, B. Tüzün, I.B. Obot, R. Touir, N. Islam, *J. Taiwan Inst. Chem. Eng.*, 65 (2016) 522-529.
20. C.D. Taylor, A. Chandra, J. Vera, N. Sridhar, *Faraday Discuss.*, 180 (2015) 459-477.
21. J. Li, X.L. Xu, K. Shi, Y. Zhou, X. Luo, Y. Wu, *Int. J. Electrochem. Sci.*, 7 (2012) 9580-9591.
22. B. Delley, *J. Chem. Phys.*, 113 (2000) 7756-7764.
23. T. Todorova, B. Delley, *Mol. Simul.*, 34 (2008) 1013-1017.
24. R.L.C. Akkermans, N.A. Spenley, S.H. Robertson, *Mol. Simul.*, 39 (2013) 1153-1164.
25. H. Sun, Z. Jin, C. Yang, R.L. Akkermans, S.H. Robertson, N.A. Spenley, S. Miller, S.M. Todd, *J Mol Model*, 22 (2016) 47.
26. L. Guo, S. Zhu, S. Zhang, Q. He, W. Li, *Corros. Sci.*, 87 (2014) 366-375.
27. J.H. Tan, L. Guo, T.M. Lv, S.T. Zhang, *Int. J. Electrochem. Sci.*, 10 (2015) 823-837.
28. T.M. Lv, S.H. Zhu, L. Guo, S.T. Zhang, *Res. Chem. Intermed.*, 41 (2014) 7073-7093.
29. Y. Qiang, L. Guo, S. Zhang, W. Li, S. Yu, J. Tan, *Scientific Reports*, 6 (2016) 33305.
30. S.S. Abdel-Rehim, K.F. Khaled, N.S. Abd-Elshafi, *Electrochim. Acta*, 51 (2006) 3269-3277.
31. L. Larabi, O. Benali, Y. Harek, *Mater. Lett.*, 61 (2007) 3287-3291.
32. Q. Qu, L. Li, S. Jiang, W. Bai, Z.T. Ding, *J. Appl. Electrochem.*, 39 (2009) 569-576.
33. H. Jafari, I. Danaee, H. Eskandari, M. RashvandAvei, *Ind. Eng, Chem, Res.*, 52 (2013) 6617-6632.
34. S.A. Ali, M.T. Saeed, S.U. Rahman, *Corros. Sci.*, 45 (2003) 253-266.
35. K.F. Khaled, *Mater. Chem. Phys.*, 112 (2008) 290-300.
36. O. Krim, A. Elidrissi, B. Hammouti, A. Ouslim, M. Benkaddour, *Chem. Eng. Commun.*, 196 (2009) 1536-1546.
37. A.U. Ezeoke, N.O. Obi-Egbedi, C.B. Adeosun, O.G. Adeyemi, *Int. J. Electrochem. Sci.*, 7 (2012) 5339-5355.
38. E.S. Ferreira, C. Giacomelli, F.C. Giacomelli, A. Spinelli, *Mater. Chem. Phys.*, 83 (2004) 129-134.
39. S. Yesudass, L.O. Olasunkanmi, I. Bahadur, M.M. Kabanda, I.B. Obot, E.E. Ebenso, *J. Taiwan Inst. Chem. Eng.*, 64 (2016) 252-268.
40. T. Koopmans, *Physica*, 1 (1934) 104-113.
41. S.B. Liu, *Acta Phys. Chim. Sin.*, 25 (2009) 590-600.
42. B. Usman, H. Maarof, H.H. Abdallah, M. Aziz, *Int. J. Electrochem. Sci.*, 10 (2015) 3223-3229.
43. C. Verma, L.O. Olasunkanrni, E.E. Ebenso, M.A. Quraishi, I.B. Obot, *J. Phys. Chem. C*, 120 (2016) 11598-11611.
44. M. Yadav, L. Gope, N. Kumari, P. Yadav, *J. Mol. Liq.*, 216 (2016) 78-86.
45. A. Kokalj, *Electrochim. Acta*, 56 (2010) 745-755.